

FIG. 4. Plots of $\tan\theta^{(1)}(\varphi)$ for protons and K mesons of energy 100 GeV for $\varepsilon_0=1$ and $\varepsilon_\varepsilon=0.001$.

$$(\varphi_{2B}^{(1)})^2 \approx \frac{1}{\operatorname{tg}^2 \theta_\infty^{(1)}} \left(\frac{1}{\mu_1^2} - \frac{1}{\mu_2^2} \right), \quad (18)$$

where $\cos\theta_\infty^{(1)} = 1/(\varepsilon_0 + \varepsilon_\varepsilon)^{1/2}$ and $\mu_{1,2} = E/m_{1,2}c^2$ is the total energy of the particle in rest-mass units ($\beta^2 = 1 - 1/\mu^2$).

The corresponding change of the angle $\theta_B^{(1)}$, which is used in ordinary Čerenkov counters to separate particles according to their masses, is

$$\Delta\theta_B^{(1)} \approx \frac{1}{2 \operatorname{tg} \theta_B^{(1)}} \left(\frac{1}{\mu_1^2} - \frac{1}{\mu_2^2} \right). \quad (19)$$

Comparing (18) and (19), it is easily seen that $\varphi_{2B}^{(1)} \gg \Delta\theta_B^{(1)}$. Figures 3 and 4 give the numerical calculation of the corresponding curves $\tan\theta^{(1)}(\varphi)$ for protons and

K mesons of energy 100 GeV.

In conclusion the authors wish to thank O. I. Sumbaev, V. A. Ruban, and A. S. Ryl'nikov for useful discussions and also L. N. Kondurova for carrying out the numerical calculations.

¹Actually, $k_\varepsilon^2/k_0^2 \equiv (n_\varepsilon^{(1,2)})^2 = (n^{(1,2)})^2 + 2\delta = \varepsilon_0 + \delta \pm (\delta^2 + \varepsilon_\varepsilon^2)^{1/2}$.

¹V. A. Belyakov and V. E. Dmitrienko, *Fiz. Tver. Tela* **15**, 2724 (1973) [*Sov. Phys. Solid State* **15**, 1811 (1974)].

²N. M. Pomerantsev, *Usp. Fiz. Nauk* **111**, 507 (1973) [*Sov. Phys. Uspekhi* **16**, 819 (1974)].

³B. W. Batterman and H. Cole, *Rev. Mod. Phys.* **36**, 681 (1964).
⁴Ya. B. Faĭnberg and N. A. Khizhnyak, *Zh. Eksp. Teor. Fiz.* **32**, 883 (1957) [*Sov. Phys. JETP* **5**, 720 (1957)].

⁵M. L. Ter-Mikaēlyan, *Izv. Akad. Nauk Armenian SSR* **14**, 103 (1961).

⁶B. M. Bolotovskii and F. N. Chukhovskii, *Zh. Eksp. Teor. Fiz.* **55**, 2011 (1968) [*Sov. Phys. JETP* **28**, 1061 (1969)].

⁷V. A. Belyakov, V. E. Dmitrienko, and V. P. Orlov, *Zh. Tekh. Fiz. Pis. Red.* **1**, 978 (1975) [*Sov. Tech. Phys. Lett.* **1**, 422 (1975)].

⁸A. I. Smirnov and V. V. Fedorov, Preprint LIYaF No. 277, 1976.

Translated by P. Millard

Two-step photoionization of helium via the $4p^1P_1$ state

M. Ya. Amus'ya, V. V. Afrosimov, V. P. Belik, S. V. Bobashev, S. A. Sheĭnerman, and L. A. Shmaenok

A. F. Ioffe Physicotechnical Institute, Academy of Sciences of the USSR, Leningrad

(Submitted 21 July 1978)

Zh. Eksp. Teor. Fiz. **76**, 873–886 (March 1979)

A new experimental method is proposed for the investigation of the photoionization of atoms from short-lived states, the excitation energy of which corresponds to the vacuum ultraviolet. The excited atoms are prepared by vacuum ultraviolet radiation from laser plasma. The technique has been used to investigate two-step photoionization of helium atoms. The ionization cross section σ_{4p} in the $4p^1P_1$ state has been measured. A theoretical analysis is given of two-step resonance photoionization in one-electron approximations, taking into account correlations between atomic electrons. Calculations of σ_{4p} in the Hartree-Fock approximation are in satisfactory agreement with the measured values, whereas the contribution of correlation processes to σ_{4p} is small.

PACS numbers: 32.80.Fb, 31.50.+w, 32.80.Kf, 52.25.Ps

1. INTRODUCTION

Considerable progress in the photoionization of atoms from the ground state has been achieved as a result of the application of new experimental techniques and the development of theoretical methods capable of taking into account many-particle effects.¹ Ionization from excited states has not been studied to the same extent despite the fact that it is of considerable interest from the

point of view of the properties of wave functions and the structure of complex atoms. Such studies are of considerable importance for applied purposes.

Direct experimental study of elementary interactions between photons and short-lived excited atoms require the use of high-intensity exciting and ionizing beams. Two-step photoionization of alkali atoms has been investigated in some isolated cases with the aid of gas-

discharge sources of high intensity radiation.² However, a much more fruitful approach has been the use of laser radiation.³⁻⁹ This has been used to investigate atoms with excitation energies of a few electron volts in the frequency range of modern tunable lasers.

It would appear at first sight that, since, in the excited state, the electron is at a relatively large distance from the core, the corresponding photoionization cross section should be similar to that of a hydrogen atom. However, calculations show that this is not the case. The ionization cross section of excited states is very different from the hydrogen cross section and, in some cases, exhibits an interesting property, namely, rapid variation near the ionization threshold, indicating that the atomic field has a very complicated structure.¹⁰ Ionization from states formed by exciting an electron from an inner shell is accompanied by the decay of the resulting vacancy and the rearrangement of all the electron shells of the atom. The cross section for this process should exhibit certain features such as oscillations, the study of which should yield information on the dynamics of electrons shell rearrangement and its effect on the wave function of the electron removed during the ionization process. Experimental data on the photoionization of excited states will enable us to verify current theoretical ideas and models used to describe atoms as complicated multiparticle systems.¹⁰⁻¹³

In this paper, we propose a new method for the experimental investigation of photoionization from short-lived atomic states, the excitation energy of which corresponds to vacuum ultraviolet. The method is based on the use of vacuum ultraviolet radiation from laser plasma to prepare the excited states. The high intensity and the continuous spectrum of the vacuum ultraviolet radiation from the laser plasma produced on a heavy metal target by a single laser pulse carrying sufficient power¹⁴⁻¹⁸ ensures that experiments with excited states of different atomic particles are now possible.

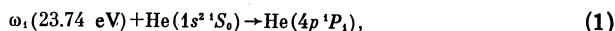
We have measured the absolute cross section for the photoionization of a helium atom from the $4p^1P_1$ state by a 1.17-eV photon. Preliminary results obtained with this new technique were reported elsewhere.¹⁹

We have also carried out a theoretical analysis of photoionization from the $4p^1P_1$ state of helium in the Coulomb and Hartree-Fock approximations, and have determined the cross section as a function of the energy of the ionizing photon in the range 1.0-1.4 eV in each of these approximations. The Hartree-Fock result is in satisfactory agreement with experimental data, whereas the result obtained in the Coulomb approximation exceeds the experimental value by a factor of more than two.

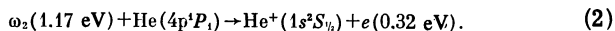
2. EXPERIMENTAL METHOD

The experimental method described below was designed for the investigation of two-step photoionization of atoms and was used to investigate the photoionization of helium from the $4p^1P_1$ state. This was done in two stages. In the first stage, the helium atom was excited by a vacuum ultraviolet photon of energy ω_1 (we use the system of units in which $\hbar = 1$) to the $4p^1P_1$ state through

the reaction

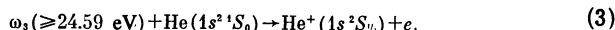


and this was followed by absorption of a photon of energy exceeding the ionization threshold in this state, with the formation of the singly-charged He^+ ion and a free electron:



The aim was to determine the absolute cross section σ_{4p} for the reaction described by (2). The helium was simultaneously exposed to two pulsed photon fluxes. The vacuum ultraviolet flux of photons with energy ω_1 was produced by passing the radiation from the laser plasma through a vacuum monochromator. The source of photons of energy ω_2 was a neodymium-glass laser. The He^+ ions produced as a result of photoionization from the excited state of helium were isolated by a time-of-flight method and were recorded.

The cross section σ_{4p} was determined in two ways. In the first method, the yield of the He^+ ions in the two-step process defined by (1) and (2) was compared with the yield of these ions in the ionization of helium from the ground state near the threshold:



In the second method, we measured the variation in the He^+ yield with increasing number of photons in the ionizing beam.

Experimental setup

The experimental setup is illustrated schematically in Fig. 1. Radiation from the Q-switched neodymium laser (1), which consisted of the generator 1a and the four-stage amplifier 1b, was directed into the vacuum chamber 8 and focussed by the objective 6 on the surface of

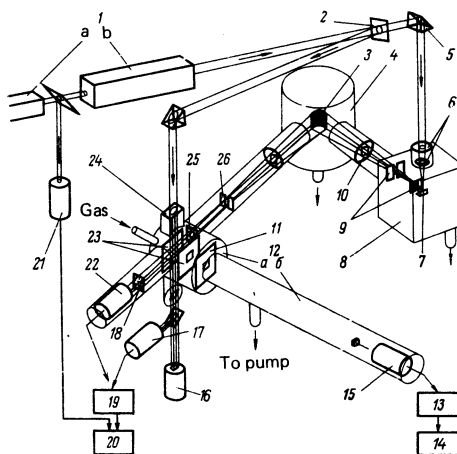


FIG. 1. Schematic illustration of apparatus: 1—Q-switched neodymium-glass laser (a—master generator, b—four-stage amplifier); 2—splitter; 3—diffraction grating; 4—vacuum monochromator; 5—rotatable prism; 6—focusing objective; 7—target; 8—vacuum chamber; 9—slits; 10—stop; 11, 23—electrodes of photoionization chamber; 12—time-of-flight mass spectrometer (a—photoionization chamber, b—drift tube); 13, 19—broadband amplifier; 14, 20—broadband oscillograph; 15—ion detector; 16—calorimeter; 17, 21—coaxial photocell; 18—attenuator; 22—vacuum ultraviolet detector; 24—ionizing beam stop; 25—vacuum ultraviolet beam stop; 26—monochromator exit slit.

the tantalum target 7. The plasma was produced by a 40-nsec, 80-J laser pulse. The energy flux density on the surface of the target in a focal spot of $\sim 150\text{-}\mu$ diameter was $10^{13} - 2 \times 10^{13} \text{ W} \cdot \text{cm}^{-2}$.

The vacuum ultraviolet radiation from the laser plasma was sent through a Seya-Namioka monochromator,²⁰ provided with a tungsten-coated toroidal diffraction grating 3. The two entrance slits 9, located at 6 and 120 mm from the laser plasma, respectively, defined the width of the region in the laser plasma from which the radiation intercepted by the diffraction grating 3 originated.¹⁾ The emerging monochromatic vacuum ultraviolet beam was collimated by the entrance window 25 of the photoionization chamber of the time-of-flight mass spectrometer 12.²² It then passed between the electrodes 23 and was detected by the VÉU-1A open electron multiplier 22. The signal from the detector 22 was received by the broad-band amplifier 19 and the output of this was applied to the broad-band storing oscillograph 20.

The beam of ionizing quanta of energy ω_2 was produced by the beam splitter 2, which diverted 8% of the energy of the main laser beam. It was then collimated by the entrance window 24 and was allowed to pass between the electrodes 23 of the photoionization chamber. The energy and time parameters of the ionizing beam were recorded by the calorimeter 16 and coaxial photocell 17.

The photoionization chamber 12a was filled with helium to a pressure $0.2 \times 10^{-4} - 2 \times 10^{-4} \text{ mm Hg}$. Simultaneous exposure to the vacuum ultraviolet and the ionizing beams in the region between the electrodes 23 produced the He^+ ions as a result of the two-step process (1), (2). The He^+ ions and the ions of the residual gas were extracted from the working volume of the photoionization chamber into the accelerating gap between the electrodes 23 and 11, and were then separated in space by a time-of-flight technique in the drift tube 12b. They eventually reached the first dynode of the detector 15 (VÉU-1A). The signal from the detector 15 was amplified and recorded by the storing oscillograph 14. The amplitude of the He^+ ion peak on the oscillogram was proportional to the yield of these ions in the photoionization process.

When the He^+ ion yield was studied as a function of the wavelength of the vacuum ultraviolet radiation in the range 49.50–54.00 nm, the amplitude of the He^+ ion peak had to be normalized because of the appreciable (20%) instability of the radiation from the laser plasma from burst to burst. Two normalization procedures were employed. In the first, the reference quantity was the signal from the detector 22. Linearity of this signal in the number of recorded quanta was ensured by reducing the intensity of the vacuum ultraviolet beam at entry to the detector by a factor of 100 with the aid of the attenuator 18. In the second method, the He^+ peak amplitude was measured simultaneously with the amplitude of one of the ion peaks due to the residual gas (O_2^+), the production cross section for which was practically constant within the vacuum ultraviolet wavelength range under investigation.²³ The ratio of these peak amplitudes at any point in the spectrum depended only on the He^+ production cross section.²⁾

Parameters of light beams

The number of vacuum ultraviolet photons traversing the photoionization chamber per pulse was measured by the method described in the literature^{24,17,18} and was found to reach $N_1 \sim 10^{11} \text{ nm}^{-1} \cdot \text{cm}^{-2}$.

The number of photons in the ionizing beam was determined by measuring its energy with the IKT-1M calorimeter, and was found to lie in the range $N_2 = 10^{17} - 10^{18}$. The readings of the IKT-1M were checked against a calibrated device for measuring the energy of laser pulses.²⁵ The uniformity of the ionizing beam was monitored with a photographic plate.

The above values of N_1 and N_2 correspond to the following fluxes of vacuum ultraviolet and ionizing radiation averaged over the corresponding pulses:

$$\bar{I}_1 \approx 2 \cdot 10^{16} \text{ nm}^{-1} \cdot \text{cm}^{-2} \cdot \text{sec}^{-1}, \quad \bar{I}_2 = 10^{26} - 10^{27} \text{ cm}^{-2} \cdot \text{sec}^{-1}.$$

The time parameters of the vacuum ultraviolet and ionizing pulses were measured with the detector 2 and coaxial FÉK=09 photocell 17, placed at equal distances from the photoionization chamber. Signals from the two detectors were first passed through the amplifier 19 and eventually received by the oscillograph 20. The pulse from the coaxial photocell 21, which was used as a reference time marker for each oscillogram, was applied to the second input of the oscillograph 20. Figure 3 (see below) shows the corresponding oscillograms of pulses due to the vacuum ultraviolet and ionizing radiation.

3. EXPERIMENTAL RESULTS

Observation of photoionization of excited helium

Figure 2 shows the He^+ yield as a function of the wavelength λ of the vacuum ultraviolet radiation in the first-order spectrum within the range 49.50–54.00 nm. The broken curve corresponds to the exposure of the gas to the vacuum ultraviolet photons alone. The appearance of the He^+ ions for $\lambda > 50.42 \text{ nm}$ is due to the ionization of helium by radiation in the second-order spectrum. For $\lambda \leq 50.42 \text{ nm}$, helium is ionized by radiation corresponding to both orders.

The solid curve in this figure shows the He^+ yield obtained by the simultaneous application of the vacuum

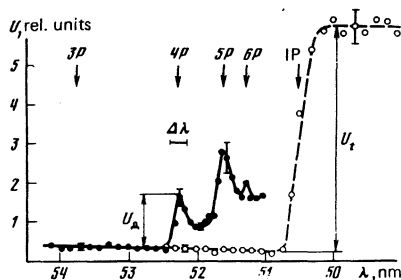


FIG. 2. Yield of singly-charged helium ions, U , as a function of wavelength λ of the vacuum ultraviolet radiation near the He absorption edge. The wavelength scale corresponds to the first-order spectrum. Broken curve—ion yield when the gas was exposed to the vacuum ultraviolet alone. Solid curve—ion yield when both the vacuum ultraviolet and ionizing beams were introduced. U_t —threshold value; IP—ionization potential.

ultraviolet and the ionizing beams. The resonance increase in the He^+ yield near $\lambda_1 = 52.22$ nm, $\lambda_2 = 51.56$ nm, and $\lambda_3 = 51.21$ nm may be regarded as evidence for the ionization of helium from the $4p^1P_1$, $5p^1P_1$, and $6p^1P_1$ states. The He^+ yield was measured with spectral resolution $\Delta\lambda = 0.25$ nm,²¹ which corresponds to the width of the $4p^1P_1$ (λ_1) peak and the absorption edge of He ($\lambda_a = 50.42$ nm). This is insufficient to resolve photoionization effects due to the $5p^1P_1$ and $6p^1P_1$ states.

Control experiments

The aim of these experiments was to show that the additional yield of helium ions, U_a (Fig. 2), was almost entirely due to the two-step photoionization from the $4p^1P_1$ state of helium, in accordance with (1) and (2). The fact that the additional helium ions appeared only in the presence of both the vacuum ultraviolet and the ionizing beams substantially reduced the range of processes capable of contributing to U_a .

1. The incidence of the ionizing beam of $10^7 \text{ W} \cdot \text{cm}^{-2}$ on the electrodes of the ionizing chamber produced the release of a large number of electrons from the metal²⁶ and these, in turn, were capable of ionizing the helium gas as a result of acceleration by the electric field between the electrodes. To suppress the secondary beam reflected from the entrance window of the photoionization chamber, the latter was located as far as possible from the electrodes 23 and was placed at an angle of 45° to the beam axis.

Periodic checks were made in the course of the experiment to verify the absence of ions from the photoionization chamber after the transmission of only the ionizing beam through it.

2. In principle, helium can be ionized from the $4p^1P_1$ state by several 1.17-eV photons. However, it is well known that a light-wave field of at least $10^5 \text{ V} \cdot \text{cm}^{-1}$ is necessary for the observation of multiphoton ionization of atoms,²⁷ whereas the electric field produced by the ionizing beam in the photoionization chamber did not exceed $5000 \text{ V} \cdot \text{cm}^{-1}$.

In accordance with the foregoing, we did not observe photoionization from the $3p^1P_1$ state of helium ($\lambda_4 = 53.74$ nm, Fig. 2), which was possible as a result of the participation of at least two photons with energy of 1.17 eV each. Since the excitation and ionization from the $3p^1P_1$ and $4p^1P_1$ states occurred under similar conditions in our experiment [equal intensities of exciting and ionizing radiation and comparable excitation probabilities: $A_{1s-3p} = 5.66 \times 10^8 \text{ sec}^{-1}$ and $A_{1s-4p} = 2.46 \times 10^8 \text{ sec}^{-1}$ (Ref. 28)] we conclude that the contribution of multiphoton processes to the ionization in the $4p^1P_1$ state can be neglected.

Determination of the absolute cross section for photoionization from the $4p^1P_1$ state of helium

It was shown above that the additional yield of He^+ ions, observed at the point $\lambda_1 = 52.22$ nm (Fig. 2) when both the vacuum ultraviolet and the ionizing beams were passed through the photoionization chamber, was exclusively due to ionization from the $4p^1P_1$ state of helium by a photon of 1.17 eV (1.06μ), i.e., the two-step process

defined by (1) and (2). Measurements of the additional yield of ions, U_a , enabled us to find the absolute cross section for the process defined by (2).

The formula for σ_{4p} was derived on the assumption that (a) the intensity of the exciting radiation was constant within the absorption line of the atom, and (b) the resonance absorption of a beam of photons of energy ω_1 and the absorption of a beam of photons of energy ω_2 along the working path in the gas were small. The balance equation for the number of helium atoms in the $4p^1P_1$ state, $n^*(t)$, which appear in a gas exposed to exciting photons of intensity $I_1(t)$ and disappear as a result of spontaneous decay of this state and its ionization by the radiation of intensity $I_2(t)$, is

$$dn^*(t)/dt = Cn_0f_{1s-4p}I_1(t) - A_{4p}n^*(t) - \sigma_{4p}I_2(t)n^*(t) \quad (4)$$

where $C = \pi e^2/mc$, n_0 is the density of atoms in the ground state, $f_{1s-4p} = 0.03$ is the oscillator strength for the $1s^{21}S_0 - 1s4p^1P_1$ transition,²⁸ and $A_{4p} = 2.55 \times 10^8 \text{ sec}^{-1}$ is the total decay probability of the $4p^1P_1$ state.²⁸ The first term on the right-hand side of this equation is the number of atoms excited per second per unit volume of the gas.²⁹

Since the intensities $I_1(t)$ and $I_2(t)$ remain sensibly constant during the lifetime of the $4p^1P_1$ state, which does not exceed 3.9 nsec (see Fig. 3), the number of excited atoms is also a slowly-varying function of time. Bearing this in mind, substituting $dn^*(t)/dt = 0$ in (4), and integrating over the time interval $t_1 - t_2$ (Fig. 3), we obtain the total number of He^+ ions accumulating per unit working volume in the photoionization chamber during the simultaneous application of the two beams:

$$n^+ = Cn_0f_{1s-4p}\sigma_{4p} \int_{t_1}^{t_2} \frac{I_1(t)I_2(t)}{A_{4p} + \sigma_{4p}I_2(t)} dt. \quad (5)$$

This equation is the starting point for the determination of the cross section σ_{4p} because the observed additional yield U_a is proportional to the number n^+ of ions:

$$U_a = k_1 n^+. \quad (6)$$

However, direct utilization of (5) and (6) is complicated by the fact that the coefficient k_1 depends on the geometry of the mutual disposition of the ionizing and exciting beams, the collection and detection efficiencies of the time-of-flight spectrometer for the He^+ ions, and the gain of the electronics. The following device was used in order to avoid measuring these parameters of the time-of-flight spectrometer and the recording system.

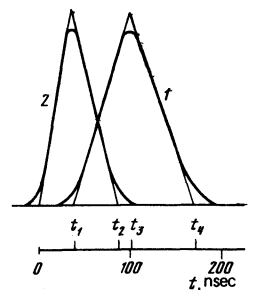


FIG. 3. Vacuum ultraviolet radiation intensity $I_1(t)$ (curve 1), the intensity $I_2(t)$ of the ionizing radiation (2), and their linear approximations.

With the monochromator adjusted for $\lambda \leq 50.42$ nm, the photon intensity $I_1(t)$ produces the following number of ions per unit volume during the time $t_1 - t_4$ of operation of the vacuum ultraviolet pulse (Fig. 3):

$$n_r^+ = \sigma_r n_0 \Delta\nu \int_{t_1}^{t_4} I_1(t) dt \quad (7)$$

and this is proportional to the quantity U_t (Fig. 2):

$$U_t = k_2 n_r^+ \quad (8)$$

where $\sigma_r = 7.5 \times 10^{-18}$ cm² is the photoionization cross section of helium near the threshold,²³ and $\Delta\nu = c\Delta\lambda/\lambda^2 = 3 \times 10^{13}$ Hz is the frequency spread of the vacuum ultraviolet radiation after the monochromator. A special control experiment was performed to determine the photoyield of Ar⁺ ions, and it was found that the intensity $I_1(t)$ of the vacuum ultraviolet photons in the photoionization chamber was practically constant within the wavelength range 49.50–54.00 nm.

For our geometry of gas illumination, $k_1 = k_2$, i.e., $U_a/U_t = n^+/n_r^+$, and the formula for σ_{4p} is as follows:

$$C\sigma_{4p} \int_{t_1}^{t_4} \frac{I_1(t)I_2(t)}{A_{1p} + \sigma_{1p}I_2(t)} dt = \sigma_r \Delta\nu \frac{U_a}{U_t} \int_{t_1}^{t_4} I_1(t) dt. \quad (9)$$

To evaluate the integrals in this expression, the functions $I_1(t)$ and $I_2(t)$ were replaced by the linear functions shown in Fig. 3. Equation (9) was then found to reduce to

$$z + z(z+1) \ln \frac{z}{z+1} + \frac{1}{2} = F \frac{U_a}{U_t}, \quad (10)$$

where

$$z^{-1} = 2\sigma_{1p}\mathcal{E}/A_{1p}t_2\omega_2s \quad (11)$$

(s is the cross-sectional area and \mathcal{E} the energy of the ionizing beam), and

$$F = \frac{\Delta\nu\sigma_r(t_4-t_1)(t_3-t_1)}{(t_3-t_1)^2 C f_{11-1p}}. \quad (12)$$

It is important to note that (10) does not involve $I_1(t)$. To determine the absolute value of σ_{4p} , we must perform an absolute determination of the time parameters of the vacuum ultraviolet and ionizing pulses and the total number of ionizing photons (energy of the ionizing beam) as well as a relative determination of U_a and U_t .

Numerical solution of (10) was used to obtain the photoionization cross section of helium from the $4p^1P_1$ state under exposure to the 1.17 eV photons. The result was $\sigma_{4p} = (15 \pm 5) \times 10^{-18}$ cm².

Another method of determining σ_{4p} , which does not involve F and U_t , is to determine the He⁺ yield as a function of the energy of the ionizing beam. This enables us to find σ_{4p} from the equation:

$$\frac{z + (z+1) [\ln z - \ln(z+1)] + 1/2}{z' + (z'+1) [\ln z' - \ln(z'+1)] + 1/2} = \frac{U_a}{U_a'}. \quad (13)$$

where U_a and U_a' is the He⁺ yield for the following two values of the energy of the ionizing beam, respectively: $\mathcal{E} \sim z$ and $\mathcal{E}' \sim z'$.

It is clear from (11) and (13) that this method of determining σ_{4p} relies on absolute measurements of \mathcal{E} , \mathcal{E}' , and t_2 (Fig. 3), and relative measurements of U_a and U_a' .

If we substitute the experimental data corresponding to $\mathcal{E} = 0.025$ J and $\mathcal{E}' = 0.1$ J in (13), we obtain the following

value (to within a factor of 2) of the cross section: $\sigma_{4p} = 1 \times 10^{-17}$ cm².

The smallest uncertainty (60%) in σ_{4p} was achieved in the first method, which is based on measurement of the ratio U_a/U_t in (10). The largest contribution to this uncertainty is due to experimental error and to fluctuations in the time parameters of the vacuum ultraviolet and ionizing pulses, and also in U_a . The point is that these quantities were not measured simultaneously in the course of the experiment and only average values were substituted in (10). When U_a is measured at the same time as the oscillograms of the two pulses are recorded (Fig. 3), the uncertainty in the result can be reduced to 30%. The choice of the energy of the ionizing beam plays a particular role. When the cross section is determined from the ratio U_a/U_t , the increase in intensity (energy \mathcal{E}) of the ionizing beam is accompanied by a monotonic increase in the uncertainty in the final result (in the limit of very large values of \mathcal{E} , the ion yield saturates, i.e., all the excited atoms are ionized and U_a is practically independent of \mathcal{E}). The beam energy ω_2 was therefore chosen to be as low as possible in the first method (sufficient to ensure that U_a lay above the noise level of the recording equipment).

The method of determining the cross section from (13) is more attractive, at least in principle, since it involves measurement of a smaller number of parameters. Its other advantage is that the experiment can be performed at higher gas pressures because resonance absorption of the exciting quanta does not, in this case, affect the final result. However, analysis shows that the use of (13) ensures final precision that is greater than in the first method but only when the width of the interval $\mathcal{E} - \mathcal{E}'$ is sufficient. In our experiments, the appearance of a background signal connected with the design features of the photoionization chamber prevented us from raising the energy in the first method above 0.15 J, whereas, to make use of the advantages of the second method, the energy must be ~ 1 J. The saturation method⁹ could not, therefore, be used to determine σ_{4p} .

4. CALCULATION OF THE CROSS SECTION FOR THE PHOTOIONIZATION OF HELIUM FROM THE $4p^1P_1$ STATE

Formulation of the problem

The photon flux density in our experiment was such that processes involving the participation of three or more photons could be neglected with a high degree of accuracy.²⁷ We shall therefore consider the two-step photoionization process in which the absorption of a photon of energy ω_1 is accompanied by a transition of an electron from the ground state of the helium atom to a real or virtual intermediate state from which the second quantum of energy ω_2 takes the system to the continuous spectrum. Figure 4 shows the simplest Feynman diagrams for this process. Summation over the excited states and integration over the continuous spectrum are assumed.

We are interested in energies of the first photon lying near the resonance energy $\omega_1 = 23.74$ eV, which corresponds to the excitation of the $4p$ level from the ground

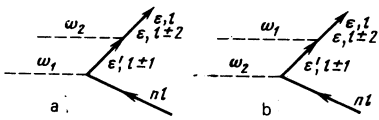


FIG. 4. Feynman diagrams for the two-step photoionization of helium.

state. In this case, the dominant contribution to the amplitude for the process is due to the transition of the electron to the $4p$ level, and the contribution of virtual states (i.e., all the terms in the sum over ϵ' with the exception of the term corresponding to the $4p$ level) can be neglected. The expression for the cross section for this process is obtained by associating a matrix element constructed in accordance with the usual correspondence rules³⁰ with the diagram of Fig. 4a, referring the transition probability to unit incident-photon flux densities, separating the angular variables, integrating with respect to angles, and summing over the components of the orbital angular momentum and the spin of the escaping electron. The final expression is

$$\sigma(\omega_1, \omega_2) = \frac{16\pi^3 e^4}{9c^2 \omega_1 \omega_2} \sum_{l_1} (E_{n_1} - E_n)^2 (\epsilon_2 - E_{n_1})^2 \left| \frac{\langle nl \| r \| n_1 l_1 \rangle \langle n_1 l_1 \| r \| \epsilon_2 l_2 \rangle}{\omega_1 - E_{n_1} + E_n + i\Gamma_{n_1 l_1} / 2} \right|^2 \quad (14)$$

where $|nl\rangle$, $|\epsilon_2 l_2\rangle$ are the initial and final states of the escaping electron in the discrete (energy E_n) and continuous (energy ϵ_2) spectra, respectively, $|n_1 l_1\rangle$ is the intermediate resonance state with energy $E_{n_1} = E_{4p}$, $\Gamma_{n_1 l_1}$ is its width, and $\langle nl \| r \| n_1 l_1 \rangle$ and $\langle n_1 l_1 \| r \| \epsilon_2 l_2 \rangle$ are the reduced dipole matrix elements in the "length form" for the $nl \rightarrow n_1 l_1$ and $n_1 l_1 \rightarrow \epsilon_2 l_2$ transitions.

The expression given by (14) must be averaged over the energy ω_1 because the width of the spectral distribution of the exciting vacuum ultraviolet radiation used in our experiment, namely, $\Delta\nu = 3 \times 10^{13}$ Hz, was much greater than the natural width of the $4p$ state ($\Gamma_{4p} = 2.55 \times 10^8$ Hz). The integration in (14) with respect to ω_1 can be carried out with the aid of the result

$$\int_{-\infty}^{\infty} \frac{d\omega_1}{|\omega_1 - \alpha + i\beta|^2} = \frac{\pi}{\beta},$$

and the final expression is

$$\sigma^r(\omega_1, \omega_2) = \sum_{l_1} \sigma_{n_1 l_1 \rightarrow n_1 l_1}(\omega_1) \sigma_{n_1 l_1 \rightarrow \epsilon_2 l_2}(\omega_2) \frac{1}{\Gamma_{n_1 l_1} \Delta E}, \quad (15)$$

where $\sigma_{n_1 l_1 \rightarrow n_1 l_1}(\omega_1)$ and $\sigma_{n_1 l_1 \rightarrow \epsilon_2 l_2}(\omega_2)$ are the single-photon ionization cross sections from the states $|nl\rangle$ and $|n_1 l_1\rangle$, respectively, and $\Delta E = 2\pi\Delta\nu$ is the energy width of the vacuum ultraviolet radiation.

According to the above estimates, the natural width of the $4p$ state is largely due to the $4p \rightarrow 1s$ radiative transition probability, so that Γ can be expressed in terms of the $nl \rightarrow n_1 l_1$ transition matrix elements as follows:

$$\Gamma_{n_1 l_1 \rightarrow n_1 l_1} = \frac{4}{3} \frac{e^2 \omega_1^3}{c^2} \frac{|\langle nl \| r \| n_1 l_1 \rangle|^2}{2l_1 + 1} \quad (16)$$

and the expression for the cross section can be written in the form

$$\sigma^r(\omega_1, \omega_2) = \sum_{l_1} \frac{2\pi^2 c^2 (2l_1 + 1)}{\omega_1^2 \Delta E} \sigma_{n_1 l_1 \rightarrow \epsilon_2 l_2}(\omega_2). \quad (17)$$

Calculation of ionization cross section

The determination of the two-photon resonance ionization cross section is thus reduced to the evaluation of the cross section for the photoionization from the excited state $|n_1 l_1\rangle$, which, in view of (14) and (15), can be written in the form

$$\sigma_{n_1 l_1 \rightarrow \epsilon_2 l_2}(\omega_2) = \frac{4}{3} \pi^2 \alpha a_0^2 \cdot 10^{18} \omega_2 |\langle n_1 l_1 \| r \| \epsilon_2 l_2 \rangle|^2, \quad (18)$$

where $\alpha = 1/137$, a_0 is the Bohr radius, and the cross section is measured in megabarns. The reduced matrix element is

$$\langle n_1 l_1 \| r \| \epsilon_2 l_2 \rangle = [(2l_1 + 1)(2l_2 + 1)]^{1/2} \begin{pmatrix} l_1 & 1 & l_2 \\ 0 & 0 & 0 \end{pmatrix} \int_0^\infty P_{n_1 l_1}(r) P_{\epsilon_2 l_2}(r) r dr, \quad (19)$$

where $P_{n_1 l_1}(r)/r$, $P_{\epsilon_2 l_2}(r)/r$ are the radial parts of the electron wave functions in the initial excited and final states, $|n_1 l_1\rangle$ and $|\epsilon_2 l_2\rangle$, respectively.

The total photoionization cross section σ_{4p} consists of the two partial cross sections $\sigma_{4p \rightarrow \epsilon d}$ and $\sigma_{4p \rightarrow \epsilon s}$ corresponding to photoionization in which the electron goes into the d or s state in the continuous spectrum, respectively:

$$\sigma_{4p} = \sigma_{4p \rightarrow \epsilon d} + \sigma_{4p \rightarrow \epsilon s}. \quad (20)$$

The formulas given by (18) and (19) were used to calculate σ_{4p} , $\sigma_{4p \rightarrow \epsilon d}$, and $\sigma_{4p \rightarrow \epsilon s}$ in the Coulomb and Hartree-Fock approximations. Calculations showed that the main contribution (about 90%) to the total cross section was provided by the $4p \rightarrow \epsilon d$ transition.

To calculate the cross section $\sigma_{4p \rightarrow \epsilon d}$ in the Coulomb approximation, the wave functions for the initial ($4p$) and final (ϵd) states were taken to be the wave functions for an electron in the screened Coulomb field due to the charge $Z_{scr} = Z - 1$.³¹ This yielded the cross section as a function of the energy of the departing electron in the range between the threshold and about 1 eV beyond the threshold. This range is fully acceptable because it includes the point $\epsilon = 0.32$ eV, which we investigated experimentally, and enabled us to obtain data that will be useful when an analogous study is performed with a tunable laser as the source of ionizing photons. The results are illustrated in Fig. 5 (curve 1). As can be seen, with increasing energy the cross section decreases quite rapidly from the threshold down to 22 Mb at $\omega_2 = 1.5$ eV. For the photon energy used in our experiment ($\omega_2 = 1.17$ eV),

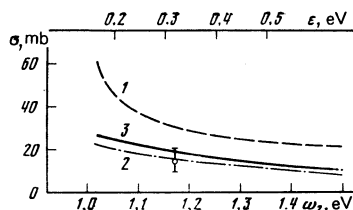


FIG. 5. Cross section for photoionization from the $4p^1P_1$ state of helium as a function of the photon energy ω_2 in the Coulomb approximation (1) and the Hartree-Fock approximation: $\sigma_{4p \rightarrow \epsilon d}^{\text{HF}}$ (3) and $\sigma_{4p \rightarrow \epsilon d}^{\text{HF}}$ (2). Points—experimental (present work). The upper scale shows the energy of the departing electron.

this cross section turns out to be $\sigma_{4p}^{\text{Coul}} = 32$ Mb. Figure 5 also shows the Hartree-Fock cross section σ_{4p}^{HF} (curve 3) and the cross section $\sigma_{4p \rightarrow \epsilon d}^{\text{HF}}$ calculated in the one-electron Hartree-Fock approximation (curve 2). In this case, the wave functions of the electron moving in accordance with the Hartree-Fock model in the self-consistent field of the core³⁰ were calculated numerically on the basis of a special program,³² and the electron in the $4p$ and ϵd states was described by functions corresponding to the motion of the excited or ionized electron in the field of the "frozen" ion with a $1s$ vacancy.³³ In the opposite case, i.e., in the determination of the wave functions for an electron removed from the $1s^2$ shell in the field of a one-electron atom with nuclear charge $Z=2$, the calculation leads to a cross section which is less than the cross section in the case of the "frozen" ion by 1%. This difference will, however, be significant when we consider ionization from inner or intermediate shells of a many-electron atom because relaxation of the outer shells during slow removal of an electron from such an atom will have an important effect on the field in which the electron moves.³⁴

The above calculations were performed for two forms of the operators involved in the interaction with the electromagnetic field, namely, length r and velocity ∇ . For exact wave functions, these two sets of results should be identical.³⁵ In the Hartree-Fock approximation, the non-local nature of the exchange potential ensures that the cross sections σ_r^{HF} and $\sigma_{\nabla}^{\text{HF}}$ are different. For $\omega_2 = 1.17$ eV, the two cross sections differ by less than 1% ($\sigma_r^{\text{HF}} = 19.63$ Mb and $\sigma_{\nabla}^{\text{HF}} = 19.57$ Mb).

Comparison with experiment

To verify that the diagrams of Fig. 4 do, in fact, describe the experimental data, we have carried out a theoretical estimate of the corrections to the amplitudes in this figure. These correlation corrections are represented by the diagrams of Fig. 6. When the photon energy ω_1 is close to the resonance value, they lead to the same final states as the processes of Fig. 4. Estimates of the contribution of the diagram of Fig. 6a show that the contribution due to the correlation between atomic electrons to the cross section $\sigma_{1s \rightarrow 4p}$ is less than 1% in the case of excitation of the $4p$ state.

Calculations of the other contributions represented by Figs. 6b-d, performed with the aid of the Hartree-Fock wave functions, show that the correlations defined by Figs. 6b and c reduce the cross section $\sigma_{4p \rightarrow \epsilon s}$ by about

20%, whereas Fig. 6d reduces the cross section $\sigma_{4p \rightarrow \epsilon d}$ by about 1%. It follows that the correlation corrections reduce the cross section σ_{4p} by about 3.5%, so that, for $\omega_2 = 1.17$ eV, the result is $\sigma_{4p} = 18.9$ Mb. This calculated value is in good agreement with the experimental result, $\sigma_{4p} = 15 \pm 5$ Mb (see Fig. 5).

Comparison of the calculated and measured results (Fig. 5) shows that the Coulomb approximation does not correctly describe the photoionization process under consideration. Satisfactory agreement with experiment can, however, be achieved within the framework of the one-electron Hartree-Fock approximation. Although the contribution due to correlation effects is small, it does bring the theoretical and experimental results closer together. The small contribution of correlation processes to the cross section (3.5%) enables us to conclude that the measured cross section is, in fact, the cross section for the ionization of the $4p$ electron moving in the self-consistent Hartree-Fock field by the photon of energy ω_2 .

We note that the ground-state photoionization cross section is much closer to the hydrogen-type cross section than is the cross section in the excited state. Hence, we may conclude that the excited state cross section is more sensitive to the choice of the theoretical model used to describe the atom. The position of the excited state is determined both by the "frozen" field of the core and by relaxation, i.e., the rearrangement of the field in the course of ionization or excitation. The influence of this rearrangement on the position of the excited state is greater than its effect on the position of the vacancy in the core. To summarize, it may be considered that measurements of excited-state photoionization cross sections, especially in the case of excitation from inner or intermediate shells, will provide a very sensitive check on theoretical models used to describe the atom.

5. CONCLUSIONS

This paper presents the first experimental and theoretical study of the photoionization of the helium atom from the $4p^1P_1$ state. We have shown that this is a two-step process. We have established that the photoionization cross section in the excited state cannot be described by the Coulomb approximation and demands the use of the more accurate Hartree-Fock wave functions.

Direct determination of the helium photoionization cross section from the state with excitation energy of 23.74 eV became possible as a result of the use of the laser plasma radiation. So far as we know, laser plasma has not been previously used as a source of vacuum ultraviolet and soft x-ray radiation for the study of elementary photon-atom interactions. The particular feature of sources of this kind (which is important for processes involving the participation of atoms in short-lived excited states) is the high photon-flux density in the continuous spectrum. As noted above, in our experiment, this density was $I = 2 \times 10^{18} \text{ nm}^{-1} \cdot \text{cm}^{-2} \cdot \text{sec}^{-1}$ at exit from the monochromator, which is higher by three or four orders of magnitude than the radiation flux density at exit from the monochromator of synchrotron ra-

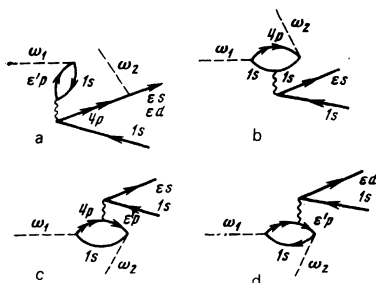


FIG. 6. Feynman diagrams for correlation processes.

diation produced by modern storage rings.³⁶ (Laser plasma cannot, however, compete with the storage ring insofar as the number of photons emitted "per working day" is concerned.) This fact enables us to look upon laser plasma as the equivalent of the yet unavailable tunable vacuum-ultraviolet laser in experiments in which the other specific properties of laser radiation are unimportant.

A natural development of our technique is to use a tunable laser to produce a beam of ionizing photons, so that a study can be made of the energy dependence of the excited-state photoionization cross sections including, in particular, the $4p^1S_0$ photoionization cross section of Ar in the near-threshold region ($\omega_2 = 2.5 - 4.0$ eV). This is of considerable interest from the theoretical point of view because this cross section undergoes a substantial variation¹⁰ near the ionization threshold, and is very sensitive to the choice of wave function. It is expected that the precision of the experimental data on the cross section will be sufficient for a choice to be made of the correct theoretical description of the process.

Studies of ionization from excited states produced as a result of the removal of an electron from an inner shell are also promising.

The authors are indebted to V. M. Dukel'skii for his interest in this research.

¹The necessity for limiting the width of the source in experiments involving resonance absorption of vacuum ultra-violet radiation from laser plasmas was demonstrated by Belik *et al.*²¹

²All the evacuated parts of the system (laser plasma chamber, monochromator, and the time-of-flight spectrometer) were pumped down to 10^{-6} mm Hg. For the working pressure of helium in the photoionization chamber, the pressure in the drift tube of the time-of-flight spectrometer did not exceed 10^{-5} mm Hg and 5×10^{-6} mm Hg elsewhere in the system. The minimum time interval between the laser radiation pulses was 5 min.

¹J. A. R. Samson, Phys. Reports C 28, 303 (1976).

²K. J. Nygaard, R. E. Hebner, J. D. Jones, and R. J. Corbin, Phys. Rev. A 12, 1440 (1975).

³V. S. Letokhov, Usp. Fiz. Nauk 118, 199 (1976) [Sov. Phys. Usp. 19, 109 (1976)].

⁴V. S. Letokhov, V. I. Mishin, and A. A. Pureskiĭ, Khim. Plazmy No. 4, 3 (1977).

⁵R. V. Ambartsumian and V. S. Letochov, Appl. Opt. 11, 354 (1972).

⁶A. N. Klyucharev and V. Yu. Sepman, Opt. Spektrosk. 38, 1230 (1975) [Opt. Spectrosc. (USSR) 38, 712 (1975)].

⁷R. V. Ambartsumyan, V. M. Apatin, V. S. Letokhov, A. A. Makarov, V. I. Mishin, A. A. Pureskiĭ, and N. P. Furzikov, Zh. Eksp. Teor. Fiz. 70, 1660 (1976) [Sov. Phys. JETP 43, 866 (1976)].

⁸D. J. Bradley, C. H. Dugan, P. Eward, and A. F. Purdic, Abstracts of Papers presented at Fourth Intern. Conf. on Atomic Physics, Heidelberg, 1976, p. 345.

⁹V. N. Ishchenko, N. V. Karlov, V. B. Krynetskiĭ, V. I. Lisitsyn, V. A. Mishin, and A. M. Razhev, Pis'ma Zh. Tekh. Fiz. 3, 1044 (1977) [Sov. Tech. Phys. Lett. 3, 428 (1977)].

¹⁰M. Ya. Amus'ya, I. S. Li, and S. I. Sheftel', Abstracts of Papers presented at All-Union Conf., Leningrad, 1977, p. 35.

¹¹A. Msezanne and S. T. Manson, Phys. Rev. Lett. 35, 364 (1975).

¹²P. G. Burke and K. T. Taylor, J. Phys. B 8, 2620 (1975).

¹³M. Ya. Amusia and N. A. Cherepkov, Case Studies in Atomic Physics 5, 47 (1975).

¹⁴A. W. Ehler and G. L. Weessler, Appl. Phys. Lett. 8, 89 (1966).

¹⁵A. W. Ehler, J. Appl. Phys. 37, 4962 (1966).

¹⁶V. A. Boiko, O. N. Krokhnin, and G. V. Sklizkov, Preprint No. 121, P. N. Lebedev Physics Institute, Academy of Sciences of the USSR, Moscow, 1971.

¹⁷V. V. Afrosimov, V. P. Belik, S. V. Bobashev, and L. A. Shmaenok, Pis'ma Zh. Tekh. Fiz. 1, 851 (1975) [Sov. Tech. Phys. Lett. 1, 370 (1975)].

¹⁸V. P. Belik, S. V. Bobashev, and L. A. Shmaenok, Abstracts of Papers presented at the Tenth Intern. Conf. on the Phys. of Elect. and Atomic Coll., Paris, 1977, p. 1286.

¹⁹V. P. Belik, S. V. Bobashev, and L. A. Shmaenok, Pis'ma Zh. Eksp. Teor. Fiz. 25, 527 (1977) [JETP Lett. 25, 494 (1977)].

²⁰J. A. R. Samson, Techniques of Vacuum Ultraviolet Spectroscopy, Wiley, New York, 1967, p. 69.

²¹V. P. Belik, S. V. Bobashev, and L. A. Shmaenok, Pis'ma Zh. Tekh. Fiz. 4, 262 (1978) [Sov. Tech. Phys. Lett. 4, 108 (1978)].

²²W. C. Wiley and J. H. McLaren, Rev. Sci. Instrum. 26, 1150 (1955).

²³J. A. R. Samson, Adv. Atomic and Molecular Phys. 2, 178 (1962).

²⁴S. V. Bobashev and L. A. Shmaenok, Inventor's Certificate No. 519 663.

²⁵V. N. Bochkarev, B. L. Vasin, V. M. Gorokhov, G. V. Sklizkov, S. I. Fedotov, and L. I. Shishkin, in: Impul'snaya fotometriya (Pulsed Photometry), Mashinostroenie, Leningrad, 1975, p. 119.

²⁶J. F. Ready, Effects of High-Power Laser Radiation, Academic Press, N.Y., 1971 (Russ. Transl., Mir, 1974).

²⁷N. B. Delone, Usp. Fiz. Nauk 115, 361 (1975) [Sov. Phys. Usp. 18, 169 (1975)].

²⁸Atomic Transition Probabilities, U.S. Department of Commerce, National Bureau of Standards, Vol. 1, 1966.

²⁹S. É. Frish, Opticheskie spektry atomov (Optical Spectra of Atoms), Vol. 5, Fizmatgiz, 1963.

³⁰D. J. Thouless, Quantum Mechanics of Many-Body Systems, Academic Press, N.Y., 1972 (Russ. Transl., Mir, 1975).

³¹H. A. Bethe and E. E. Salpeter, Quantum Mechanics of One and Two Electron Atoms, Springer Verlag, Berlin, 1957.

³²L. V. Chernysheva, N. A. Cherepkov, and V. Radoevich, Preprint No. 487, Physicotechnical Institute, 1975.

³³M. Ya. Amus'ya, N. A. Cherepkov, and L. V. Chernysheva, Zh. Eksp. Teor. Fiz. 60, 160 (1971) [Sov. Phys. JETP 33, 90 (1971)].

³⁴M. Ya. Amus'ya, S. A. Sheĭnerman, and S. I. Sheftel', Zh. Tekh. Fiz. 47, 1432 (1977) [Sov. Phys. Tech. Phys. 22, 822 (1977)].

³⁵M. Inocuti, Rev. Mod. Phys. 43, 297 (1971).

³⁶S. V. Bobashev, Proc. Third All-Union School on the Physics of Electronics and Atomic Collisions, Institute of Nuclear Physics, Leningrad, 1976, p. 39.

Translated by S. Chomet